Progress and plans for the study of sawteeth, helical states, and snakes with M3D-C[1]

S. C. Jardin[1]
N.M. Ferraro[2], J. Breslau[1,] J. Chen[1],

[1]*Princeton Plasma Physics Laboratory*
[2] *General Atomics*

CEMM Meeting
Providence, Rhode Island
28-Oct-2012
Westin Providence-Rhode Island Convention Center
Providence Ballroom I/IV

This work was performed in close collaboration with M. Shephard, F. Zhang, and F. Delalondre at the SCOREC center at Rensselaer Polytechnic Institute in Troy, NY.

Acknowledgements also to: M. Chance, G. Fu, S. Hudson, H. Strauss, L. Sugiyama

PPPL PRINCETON PLASMA PHYSICS LABORATORY

Outline

- Applications
  - Overview
  - DIII
  - NSTX
  - ITER
- Algorithm Improvements
  - "more implicit" field advance
  - 2F algorithm improvements
- Summary

Application Campaign: What limits q_0 in an ohmic discharge?

- resistive or 2F MHD
- can take very long time steps $\Delta t \sim 10\text{-}100\ \tau_A$
  - total simulation time up to 10^5 or $10^6\ \tau_A$
- free-boundary
  - plasma can be separatrix limited
  - plasma is surrounded by low-temperature plasma "vacuum"
  - simulation domain is interior to vacuum vessel
- need to specify:
  - transport model (η, μ, χ)
  - sources for energy and particles
  - loop-voltage on vacuum vessel
    - with controller to maintain plasma current

PPPL PRINCETON PLASMA PHYSICS LABORATORY

Depending on the transport model: sawteeth or internal helical states

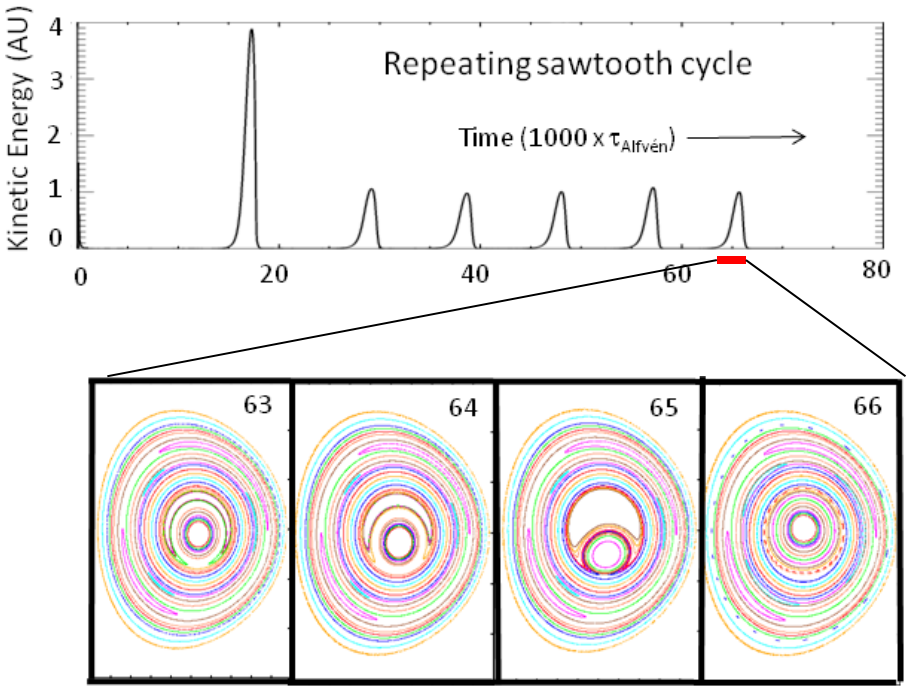

Some transport models and geometry lead to periodic sawtooth oscillations. Shown here are 6 sawtooth events (only first depends on initial conditions). Bottom shows Poincare plots at 4 times indicated.

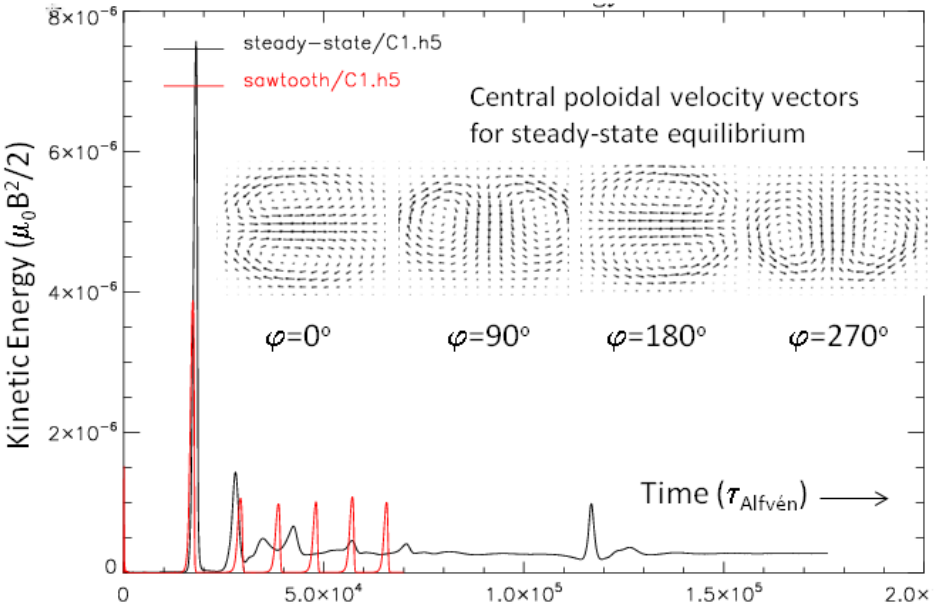

Other transport models lead to stationary states with helical structures and flows (viscosity reduced by 3 in black curve)

PPPL PRINCETON PLASMA PHYSICS LABORATORY

DIII-D
Comparison of D-shaped and elliptical

We have compared the simulated sawtooth behavior of two discharges with very similar parameters but with differing cross-sectional shapes.

- The kinetic energy peak for the dee-shaped plasma is about 10 times that of the elliptical shaped plasma

- Likely explained by the larger region in the dee-shaped plasma that reconnects. The q-profile can decrease to a lower value before the plasma is sufficiently unstable to initiate a reconnection event.

PPPL PRINCETON PLASMA PHYSICS LABORATORY

Peak KE for Dee-shaped plasma ~ 10x that of ellipse

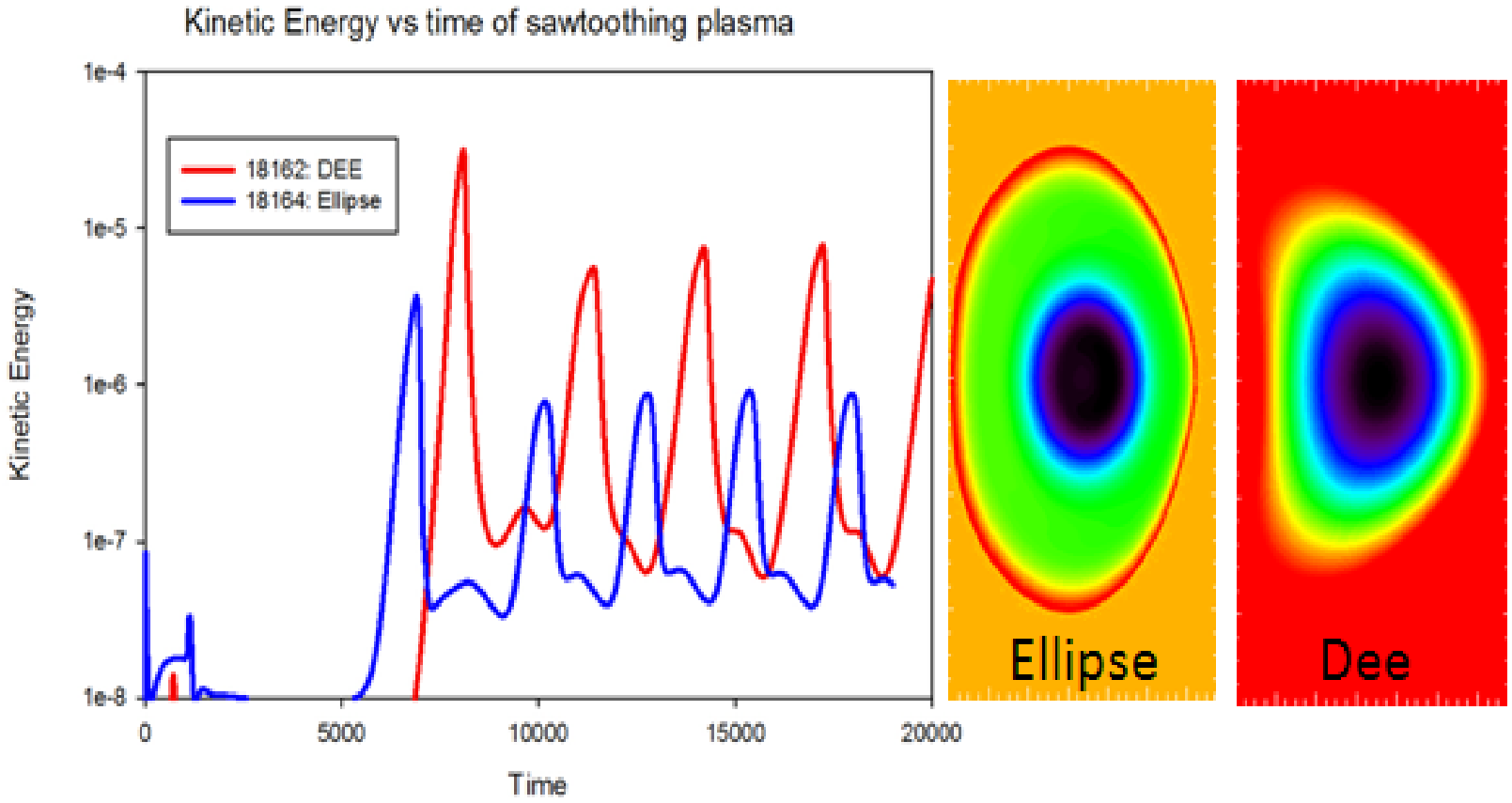

Same transport model used for both

Poincare plots for elliptical plasma calculation

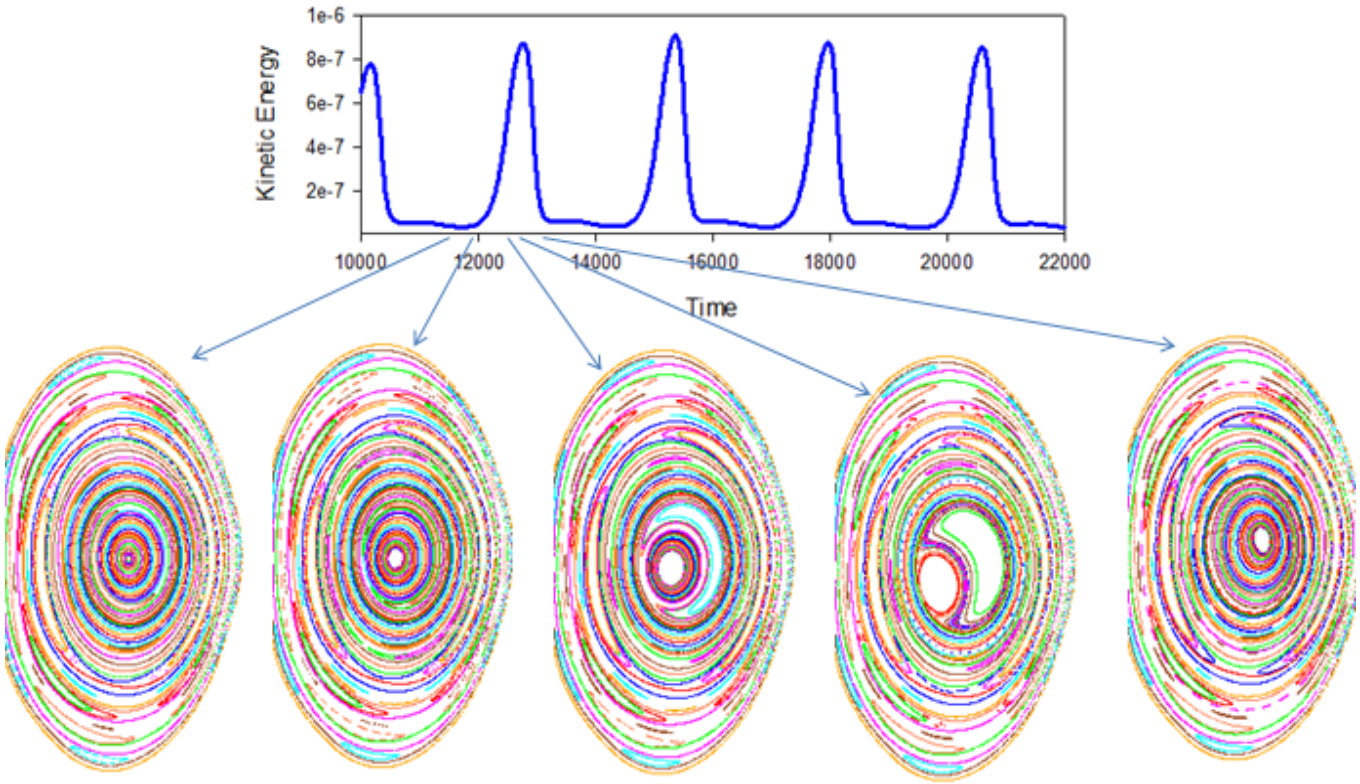

Relatively small reconnection region

Poincare plots for dee-shaped plasma calculation

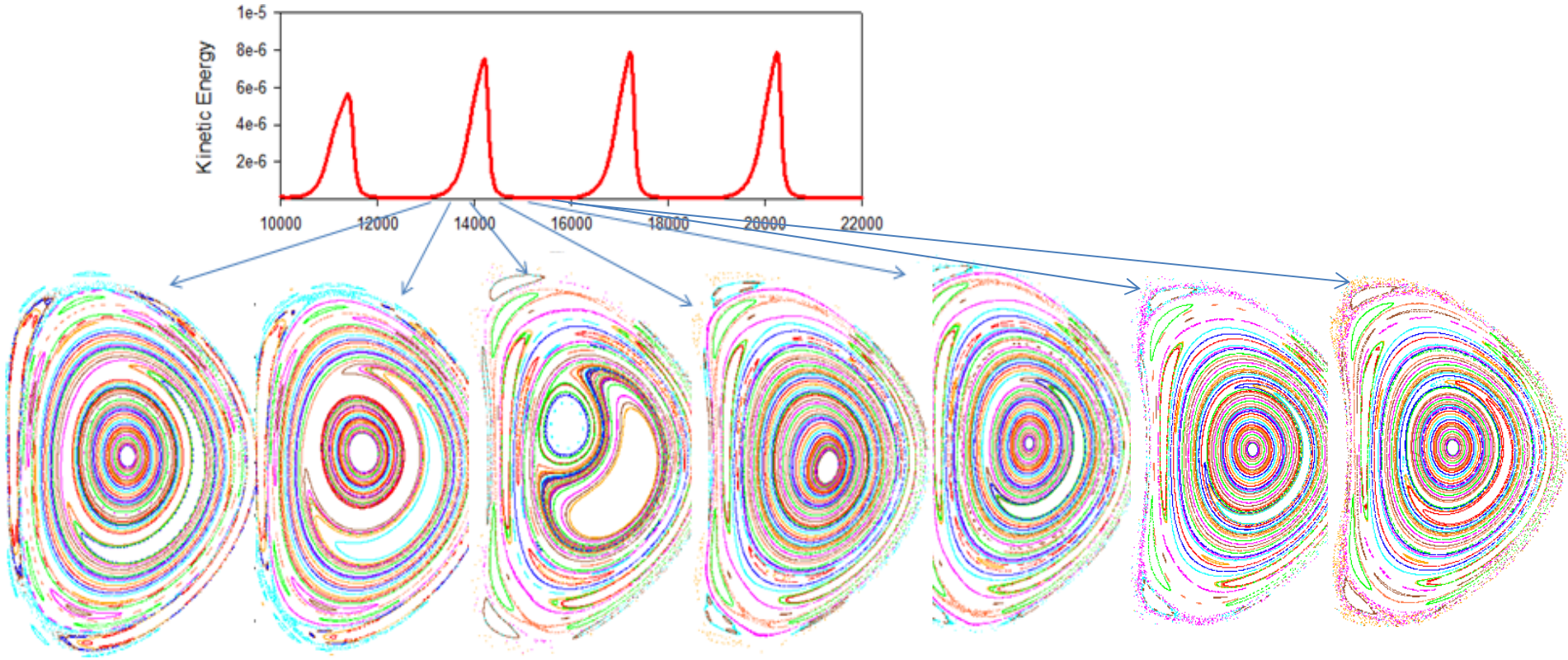

Much larger reconnection region

Note: m=1 island persists for the entire cycle: SNAKE!

Comparison of q-profiles

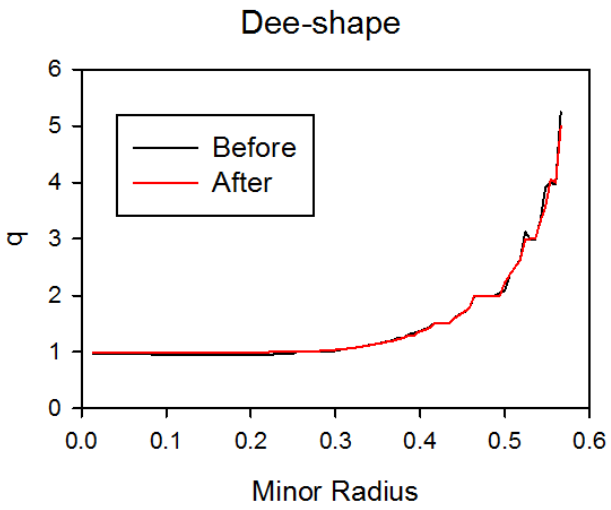

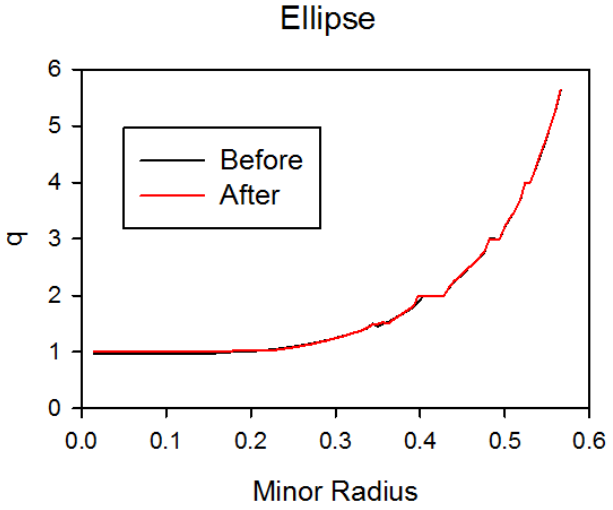

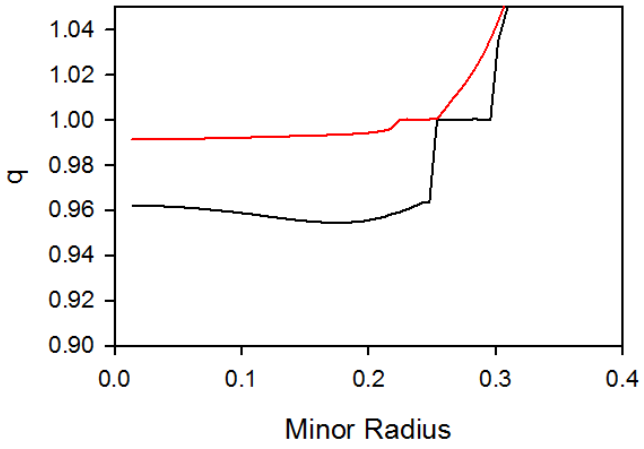

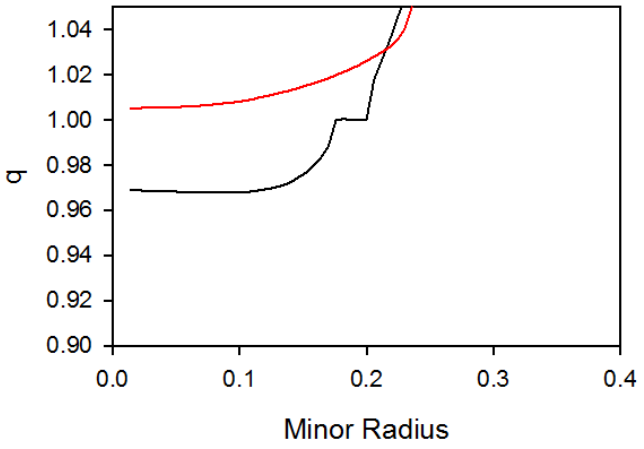

Comparison of pressure-profiles

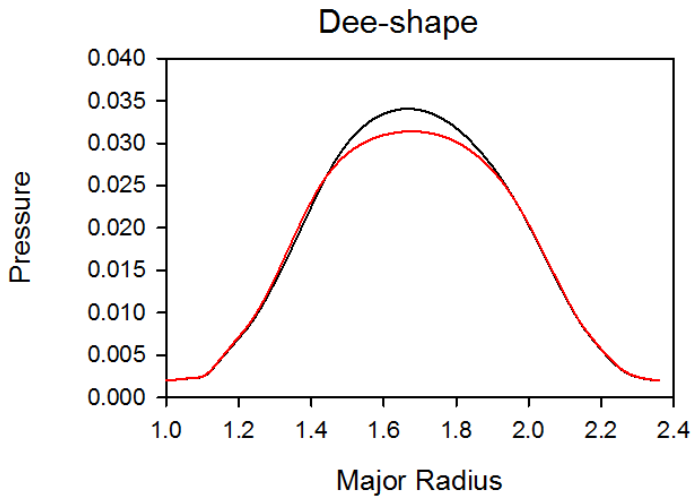

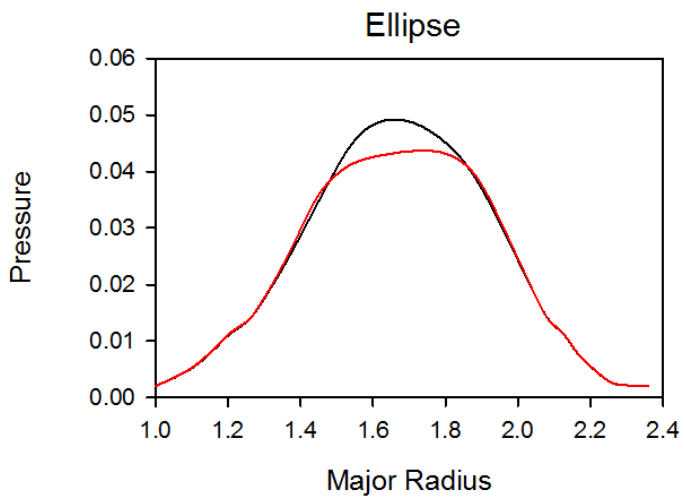

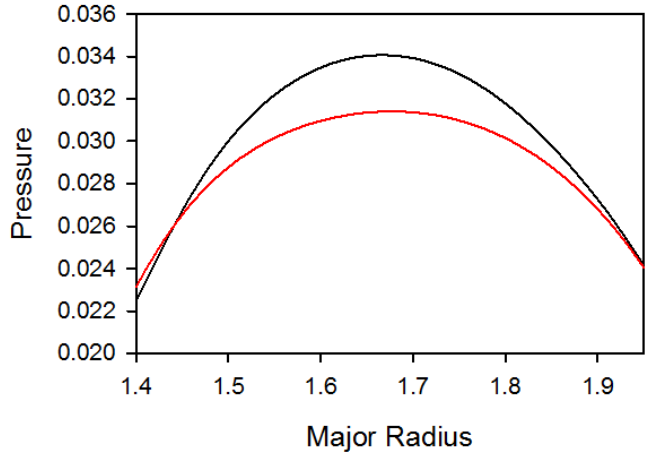

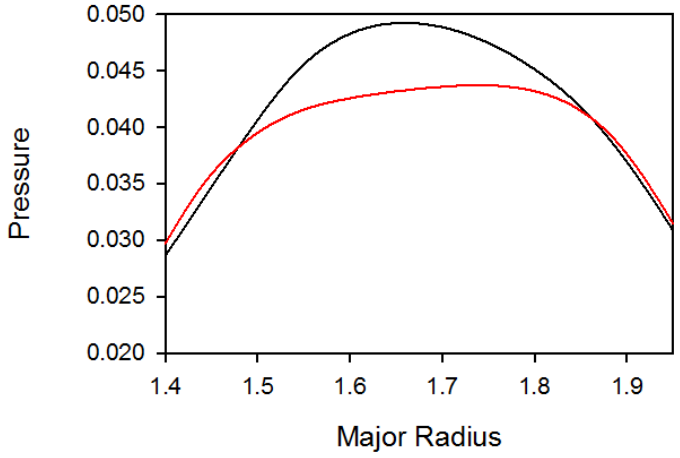

We suspect there are 3 timescales that scale differently with resistivity

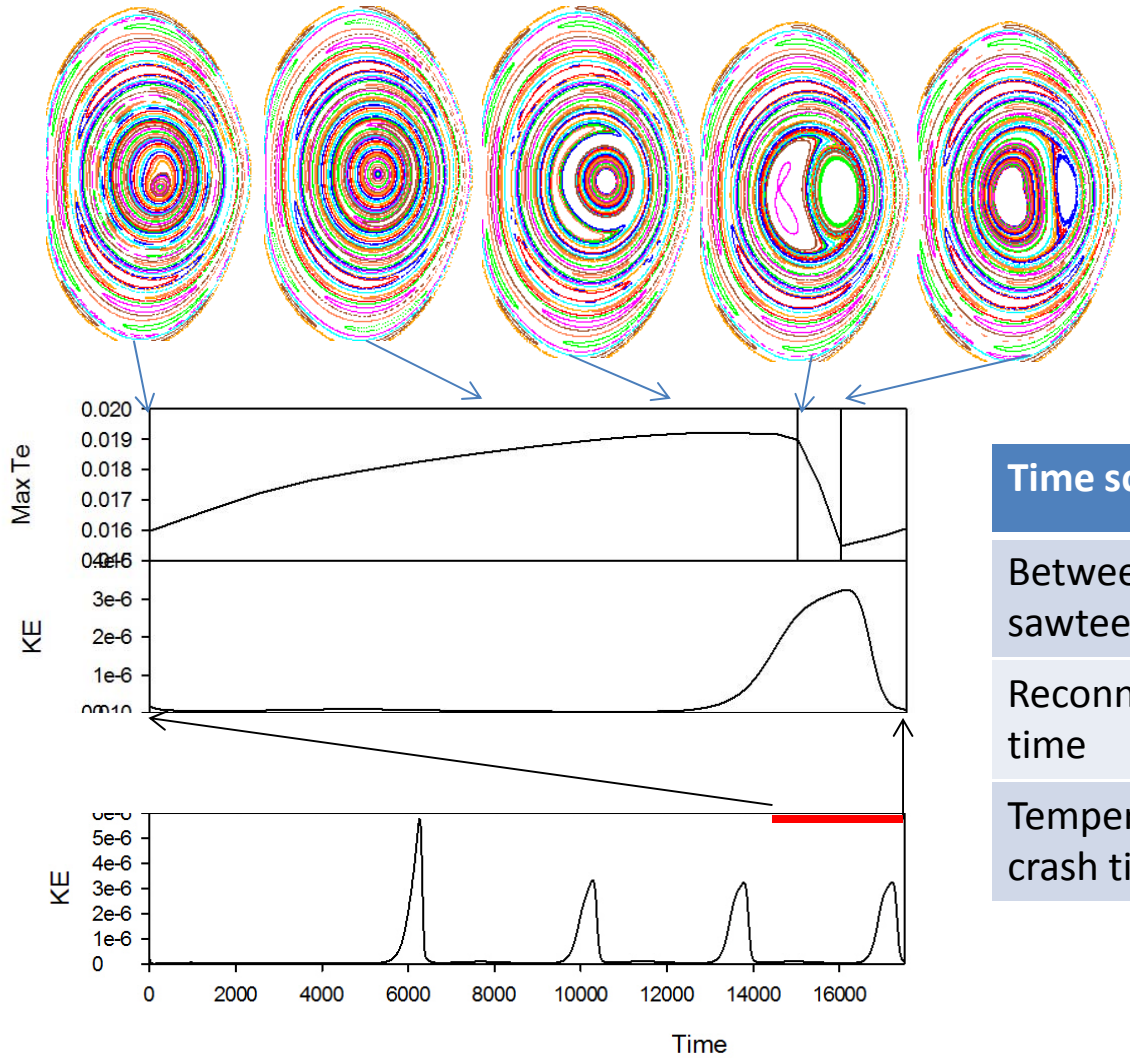

The temperature crash is very short compared to the reconnection time.

We are now performing scaling studies to verify this.

Time scale	value	scaling
Between sawteeth	10,000 τ_A	η ?
Reconnection time	1,000 τ_A	$\eta^{1/2}$?
Temperature crash time	200 τ_A	η^0 ?

NSTX
Study of the "long-lived" mode

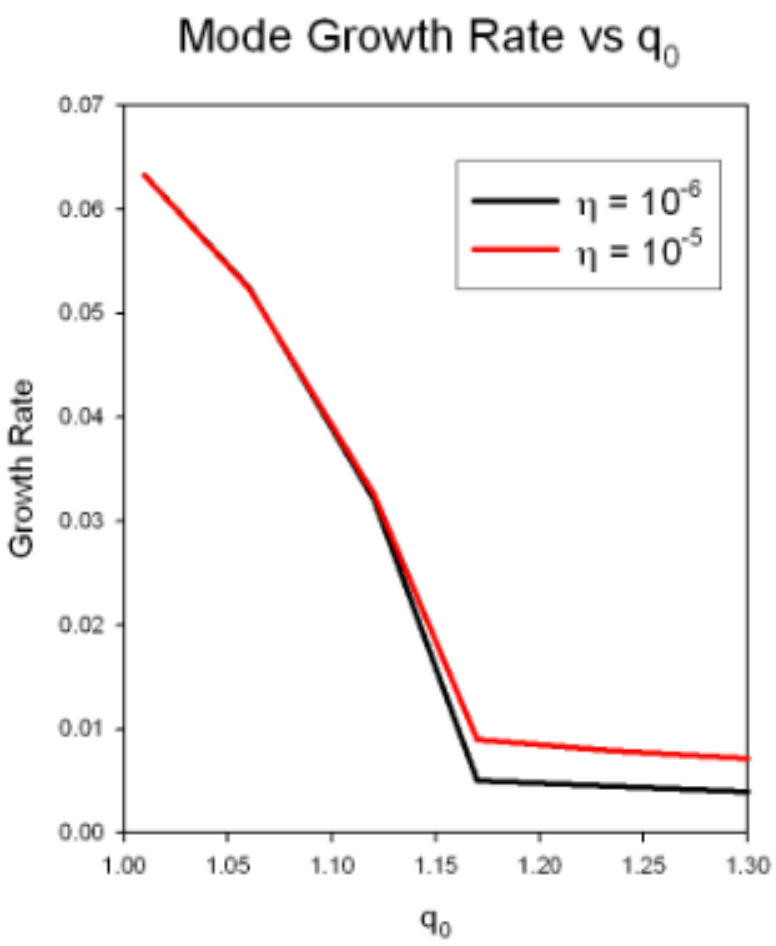

At the 2010 IAEA meeting, Breslau studied the nonlinear behavior of a series of equilibrium that were obtained by "Bateman Scaling" an EFIT reconstruction of an experimental equilibrium.

It was found that a saturated n=1, m=1,2 mode would appear for q0 low enough.

Here we are trying to reproduce this more self-consistently by time-evolving the initial equilibrium

NSTX
Comparison of the q-profiles

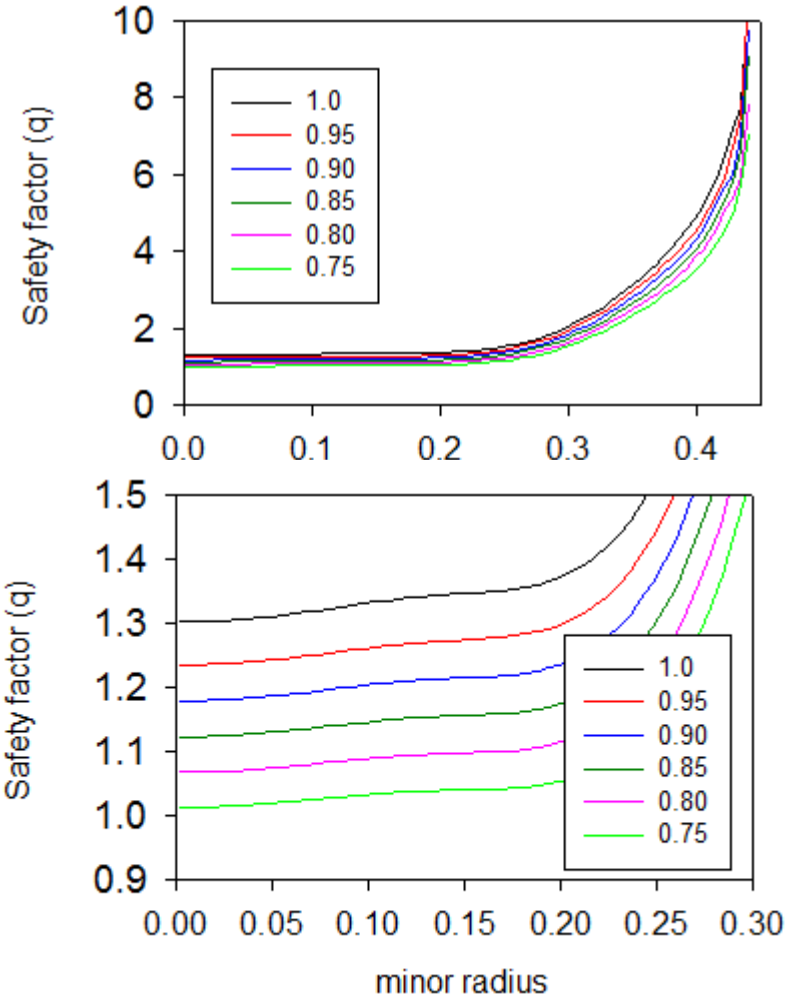

Bateman scaled q-profiles

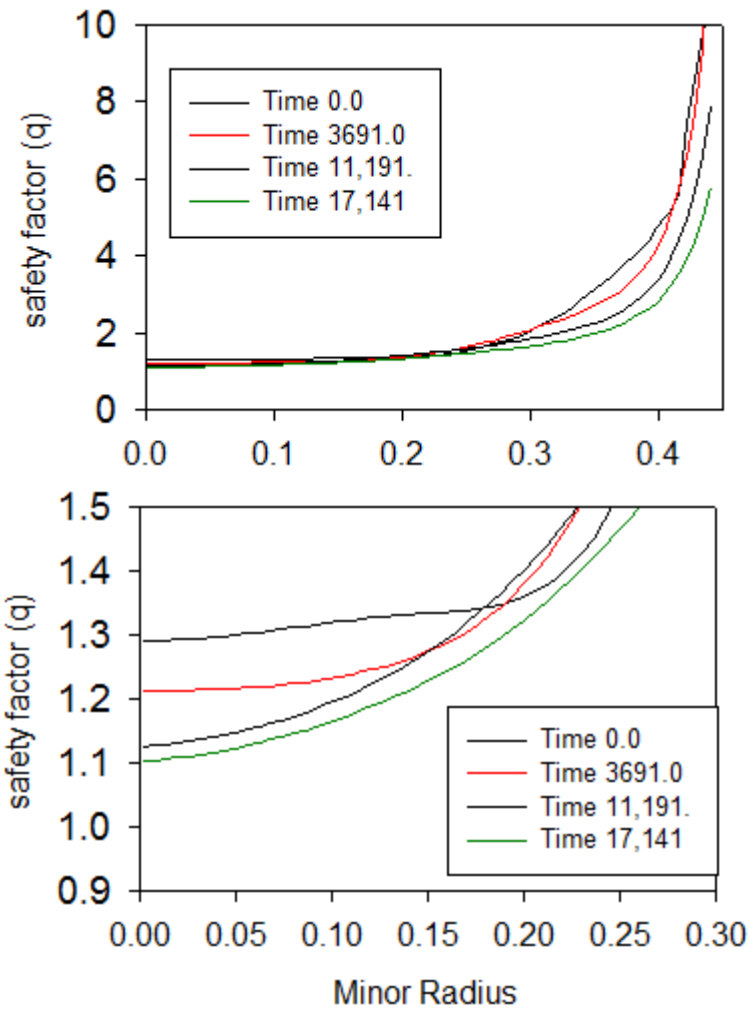

Time evolved q-profiles

NSTX
Status of the time-evolution run

Calculation is still running on the PPPL local cluster, but has not yet developed any non-axisymmetric instability.

Presently has t= 18,000 τ_A with q_0 = 1.10

Likely difference between the "Bateman scaled" equilibrium is the difference in the central shear…much greater in this series.

Likely need to include NBCD in calculation to get correct q-profile evolution

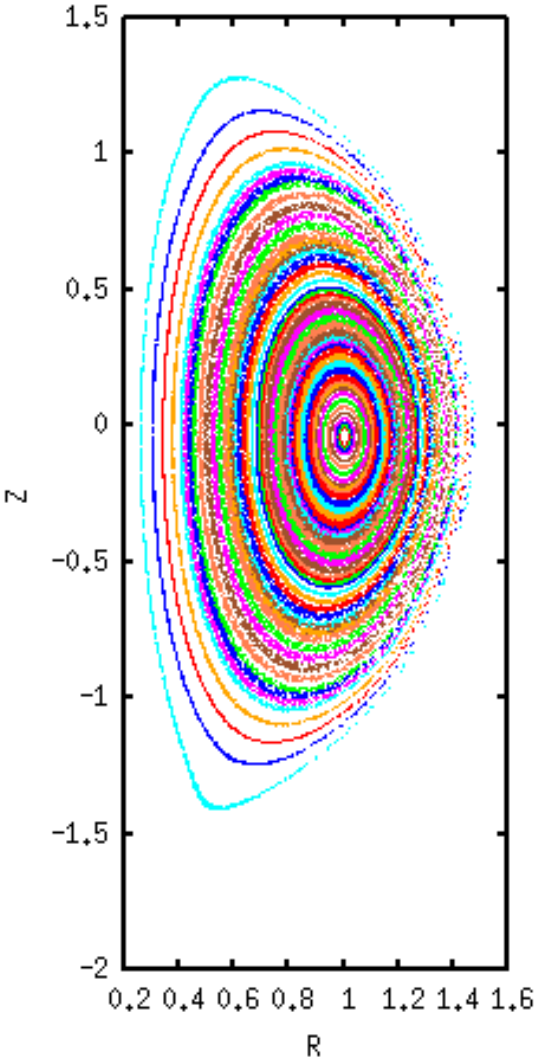

ITER calculation still in progress. Partial reconnection has occured

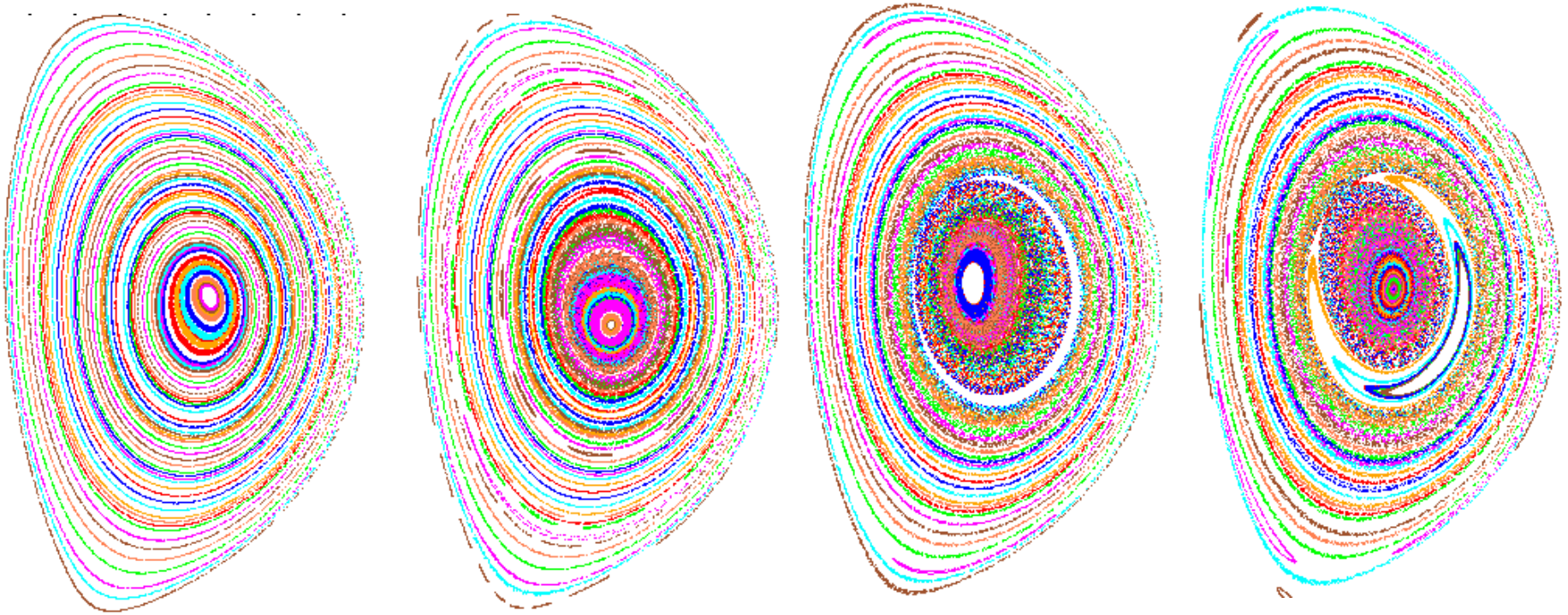

T=13,622 τ_A
$\beta(0) = 0.087$

T=17,622 τ_A
$\beta(0) = 0.087$

T=20,622 τ_A
$\beta(0) = 0.077$

T=24,622 τ_A
$\beta(0) = 0.070$

Poincare plots

PPPL
PRINCETON
PLASMA PHYSICS
LABORATORY

Internal mode has not yet affected plasma boundary…but still developing

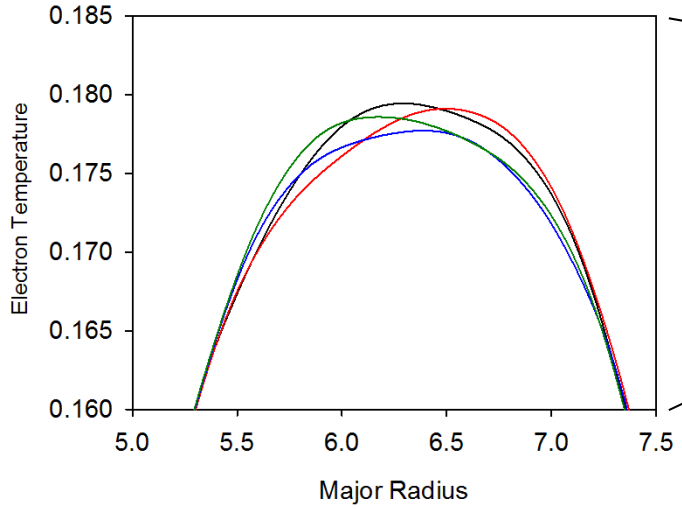

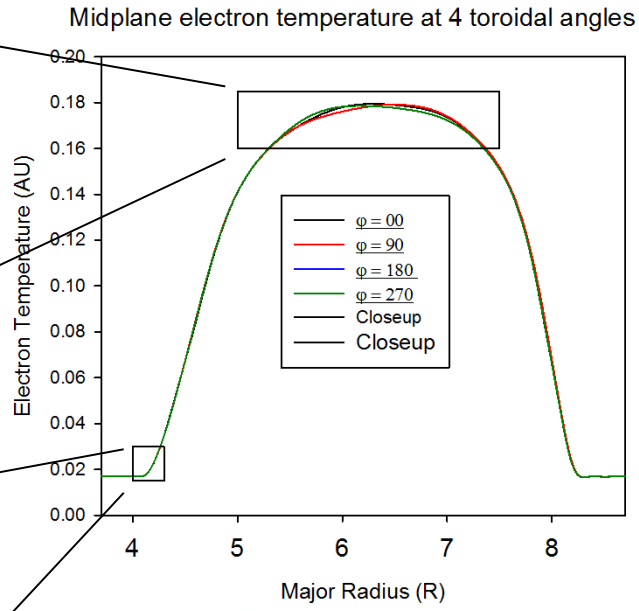

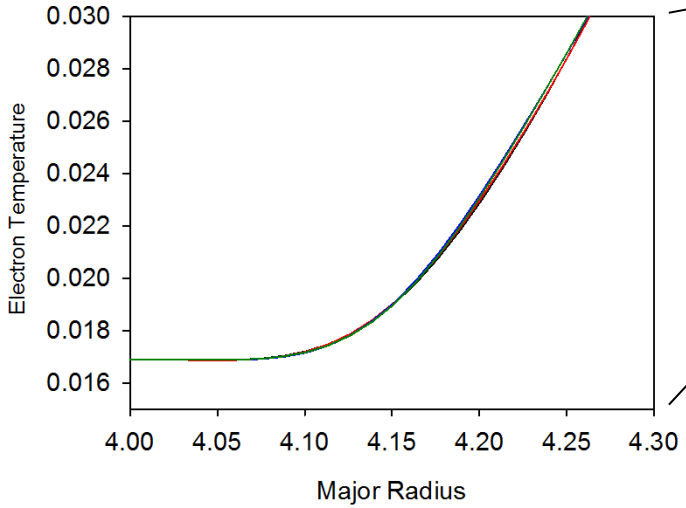

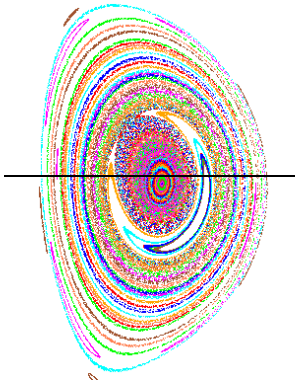

PPPL PRINCETON PLASMA PHYSICS LABORATORY

2F Ohm's law in M3D-C^1

There are two forms of the 2F Ohm's law that are mathematically equivalent:

$$\frac{\partial \mathbf{B}}{\partial t} = \nabla \times \left[\mathbf{u} \times \mathbf{B} - \eta \mathbf{J} - \frac{1}{ne}\left(\mathbf{J} \times \mathbf{B} - \nabla p_e - \nabla \bullet \boldsymbol{\Pi}_e \right) \right]$$

Electron form

$$\frac{\partial \mathbf{B}}{\partial t} = \nabla \times \left[\mathbf{u} \times \mathbf{B} - \eta \mathbf{J} - \frac{M_i}{e}\left(\frac{\partial \mathbf{u}}{\partial t} + \mathbf{u} \bullet \nabla \mathbf{u} \right) - \frac{1}{ne}\left(\nabla p_i + \nabla \bullet \boldsymbol{\Pi}_i \right) \right]$$

Ion form

- We have implemented both of these forms in M3D-C1
  - to serve as a check….can we get same result?
  - to determine which has better convergence properties in 3D

2-fluid split algorithm

Recall the split algorithm consists of a velocity solve followed by separate solves for the fields, the temperatures, and the density.

$$\begin{bmatrix} U \\ \omega \\ \chi \end{bmatrix}^{n+1} \rightarrow \begin{bmatrix} \psi \\ F \\ f \end{bmatrix}^{n+1} + \begin{bmatrix} T_e \\ T_i \end{bmatrix}^{n+1} + \left[n \right]^{n+1}$$

1. How is the velocity solve modified by 2F terms ?
2. How is the magnetic field solve modified by 2F terms?

$$\mathbf{V} = R^2 \nabla U \times \nabla \varphi + \boldsymbol{\omega} R^2 \nabla \varphi + R^{-2} \nabla_\perp \chi$$

$$\mathbf{B} = \nabla \psi \times \nabla \varphi - \nabla_\perp f' + F \nabla \varphi : \qquad \nabla_\perp^2 f = F - F_0$$

$$p_e = nT_e \quad \& \quad p_i = nT_i$$

ion form of 2-fluid velocity solve

$$nM_i\dot{\mathbf{V}} = \left(\mathbf{J} + \theta\delta t\left(\nabla\times\dot{\mathbf{B}}\right)\right)\times\left(\mathbf{B} + \theta\delta t\dot{\mathbf{B}}\right) - \nabla\left(p + \theta\delta t\dot{p}\right) + \cdots$$

$$\dot{\mathbf{B}} = \nabla\times\left[\left(\mathbf{V} + \theta\delta t\dot{\mathbf{V}}\right)\times\mathbf{B} - \frac{M_i}{e}\left(\dot{\mathbf{V}} + \mathbf{V}\bullet\nabla\mathbf{V}\right) - \frac{1}{ne}\left[\nabla p_i + \nabla\bullet\Pi_i\right] + \cdots\right]$$

–Ion velocity form for 2F differential approximation operator

2F Implicit velocity advance becomes:

$$\left(nM_i - \theta^2\delta t^2 L_0 + \theta\delta t d_i L_1\right)\mathbf{V}^{n+1} = \left(nM_i + \theta\left(\theta - 1\right)\delta t^2 L_0 + \theta\delta t d_i L_1\right)\mathbf{V}^n + \cdots$$

Here, the two operators are defined as:

$$L_0\left\{\mathbf{V}\right\} = \left\{\nabla\times\left[\nabla\times\left(\mathbf{V}\times\mathbf{B}\right)\right]\right\}\times\mathbf{B} + \left(\nabla\times\mathbf{B}\right)\times\left[\nabla\times\left(\mathbf{V}\times\mathbf{B}\right)\right] + \nabla\left(\mathbf{V}\bullet\nabla p + \gamma p\nabla\bullet\mathbf{V}\right)$$

$$L_1\left\{\mathbf{V}\right\} = \left\{\nabla\times\left[\nabla\times\mathbf{V}\right]\right\}\times\mathbf{B} + \left(\nabla\times\mathbf{B}\right)\times\left[\nabla\times\mathbf{V}\right]$$

Magnetic field solve with ion form

$$\frac{\partial}{\partial t}\left(\nabla\times\mathbf{A}\right)=\nabla\times\left[\mathbf{u}\times\mathbf{B}-\eta\mathbf{J}-\frac{M_i}{e}\left(\frac{\partial\mathbf{u}}{\partial t}+\mathbf{u}\bullet\nabla\mathbf{u}\right)-\frac{1}{ne}\left(\nabla p_i+\nabla\bullet\boldsymbol{\Pi}_i\right)\right]$$

$$\frac{\partial\mathbf{A}}{\partial t}=\mathbf{u}\times\mathbf{B}-\eta\mathbf{J}-\frac{M_i}{e}\left(\frac{\partial\mathbf{u}}{\partial t}+\mathbf{u}\bullet\nabla\mathbf{u}\right)-\frac{1}{ne}\left(\nabla p_i+\nabla\bullet\boldsymbol{\Pi}_i\right)+\nabla\Phi$$

Note that time derivatives of $\mathbf{A}$ and $\mathbf{u}$ enter in a similar way. This is facilitated by the form taken for the velocity and the vector potential in M3D-C^1

$$\mathbf{u}=R^2\nabla U\times\nabla\varphi+\boldsymbol{\omega}R^2\nabla\varphi+R^{-2}\nabla_\perp\chi$$

$$\mathbf{A}=-R^2\nabla f\times\nabla\varphi+\psi\nabla\varphi$$

Thus, we have: $\dot{f}\rightarrow\dot{f}-\frac{M_i}{e}\dot{U},\quad\dot{\psi}\rightarrow\dot{\psi}+\frac{M_i}{e}R^2\dot{\omega}$

For electron form, introduce Harned-Mikic terms

$$\frac{1}{R^2}\dot{F} = \nabla_\perp \bullet \left[-F\nabla_\perp U \times \nabla\varphi + \omega\nabla_\perp \psi \times \nabla\varphi - \frac{1}{R^4} F\nabla_\perp \chi - \omega\nabla_\perp f' \right]$$
$$+\nabla_\perp \bullet \eta \left[\frac{1}{R^2}\nabla F^* - \frac{1}{R^2}\nabla_\perp \psi' \times \nabla\varphi \right]$$
$$+d_i \nabla_\perp \bullet \left[\frac{1}{\rho R^2}\Delta^*\psi\nabla_\perp\psi \times \nabla\varphi + \frac{F}{\rho R^2}\nabla_\perp F^* \times \nabla\varphi + \frac{1}{\rho}\nabla_\perp p_e \times \nabla\varphi + \frac{F}{\rho R^4}\nabla_\perp \psi' - \frac{1}{\rho R^2}\Delta^*\psi\nabla_\perp f' \right]$$

$$\nabla_\perp \bullet \frac{1}{R^2}\nabla\dot{\psi} = \nabla_\perp \bullet \frac{1}{R^2}\nabla r^2[U,\psi] - \nabla_\perp \bullet \frac{1}{R^2}\nabla r^2(U, f') + \nabla_\perp \cdot \left[\frac{F}{R^2}\nabla_\perp U \right]' - \nabla_\perp \cdot \left[\frac{\omega}{R^2}\nabla_\perp\psi + \omega\nabla_\perp f' \times \nabla\varphi \right]'$$
$$-\nabla_\perp \bullet \frac{1}{R^2}\nabla r^{-2}(\chi,\psi) - \nabla_\perp \bullet \frac{1}{R^2}\nabla R_0^2[\chi, f'] - \nabla_\perp \cdot \left[\frac{F}{r^2R^2}\nabla_\perp \chi \times \nabla\varphi \right]'$$
$$+\nabla_\perp \bullet \frac{1}{R^2}\nabla\eta\Delta^*\psi + \nabla_\perp \cdot \left[\frac{\eta}{R^2}\nabla F^* \times \nabla\varphi + \frac{\eta}{R^4}\nabla_\perp\psi' \right]'$$
$$+\nabla_\perp \bullet \frac{1}{R^2}\nabla \frac{d_i}{\rho}\left[[\psi, F^*] + (F^*, f') + \frac{1}{R^2}(\psi,\psi') + [\psi', f'] + p_e' \right]$$
$$-\nabla_\perp \cdot d_i \left[\begin{array}{l} \frac{1}{R^4\rho}\Delta^*\psi\nabla_\perp\psi + \frac{F}{R^4\rho}\nabla_\perp F^* + \frac{1}{R^2\rho}\nabla_\perp p_e \\ -\frac{F}{R^4\rho}\nabla_\perp\psi' \times \nabla\varphi + \frac{1}{R^2\rho}\Delta^*\psi\nabla_\perp f' \times \nabla\varphi \end{array} \right]'$$

$$(\ )' \equiv \frac{\partial}{\partial\varphi}(\ )$$

$$\mathbf{B} = \nabla\psi \times \nabla\varphi$$
$$-\nabla_\perp f' + F\nabla\varphi$$

$$\nabla_\perp^2 f = F - F_0$$

Dominant cross terms in field advance are marked in red

Harned-Mikic terms -- 2

Implicit advance for the field variables have the Harned-Mikic terms added to make the matrix more diagonal and improve the 3D iterative solution when 2F terms are present.

$$\nabla_\perp \bullet \frac{1}{R^2} \nabla_\perp \dot{\psi} + \left(\theta \delta t \, d_i\right)^2 (H_m) \nabla_\perp \bullet \underbrace{\left[\frac{F}{R^4 n} \nabla_\perp \left(R^2 \nabla_\perp \bullet \frac{F}{R^4 n} \nabla_\perp \dot{\psi}'' \right) \right]}_{\left(\mathbf{B}\bullet\nabla\right)^2 \nabla_\perp^2} = \cdots$$

$$\frac{1}{R^2} \dot{F} + \left(\theta \delta t \, d_i\right)^2 (H_m) \underbrace{\frac{F}{nR^2} \nabla_\perp \bullet \frac{F}{nR^4} \nabla_\perp \dot{F}''}_{\left(\mathbf{B}\bullet\nabla\right)^2 \nabla_\perp^2} = \cdots$$

Eigenvalues of the field matrix after preconditioning (with no HM terms)

$d_i = 0$

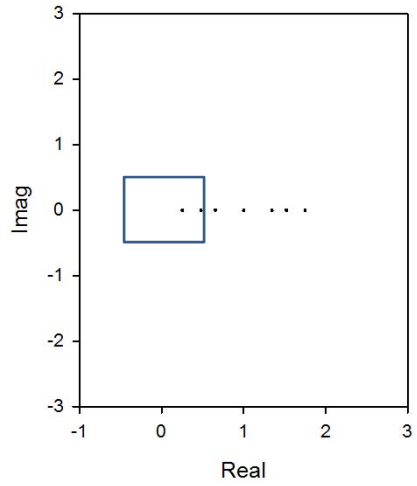

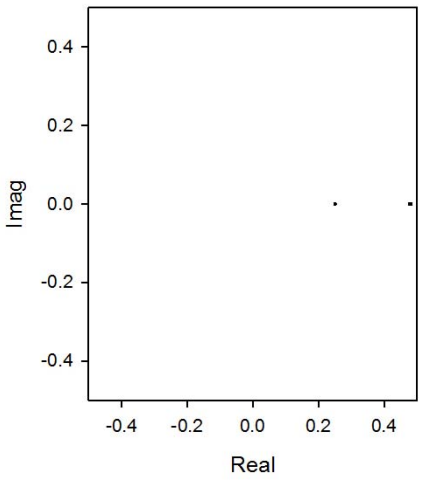

$d_i = .045$

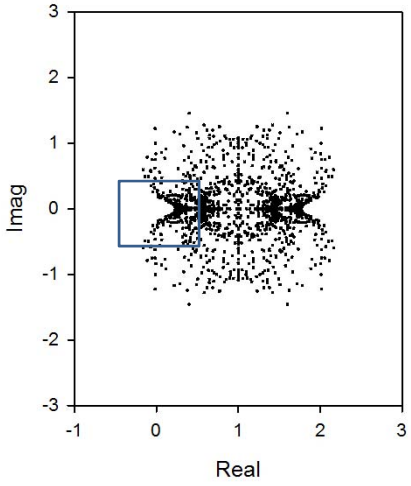

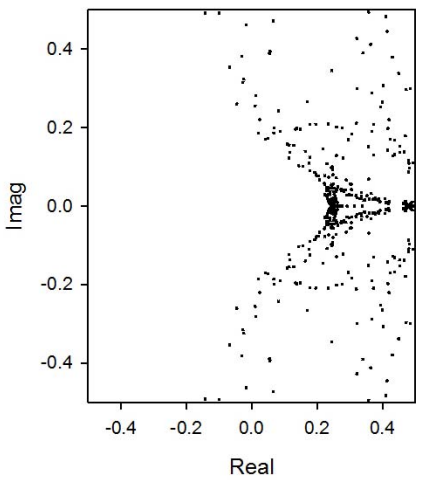

$d_i = .090$

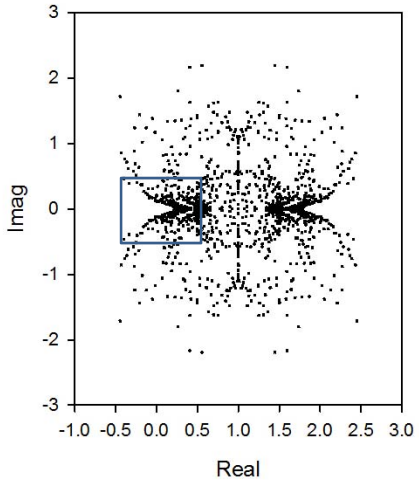

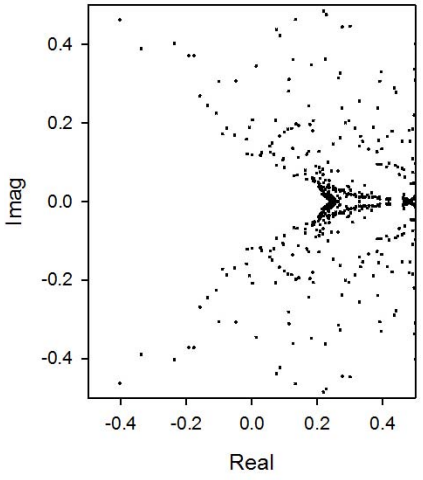

Eigenvalues of the field matrix with d_i=.09 after preconditioning showing the effect of the Harned-Mikic terms (in red)

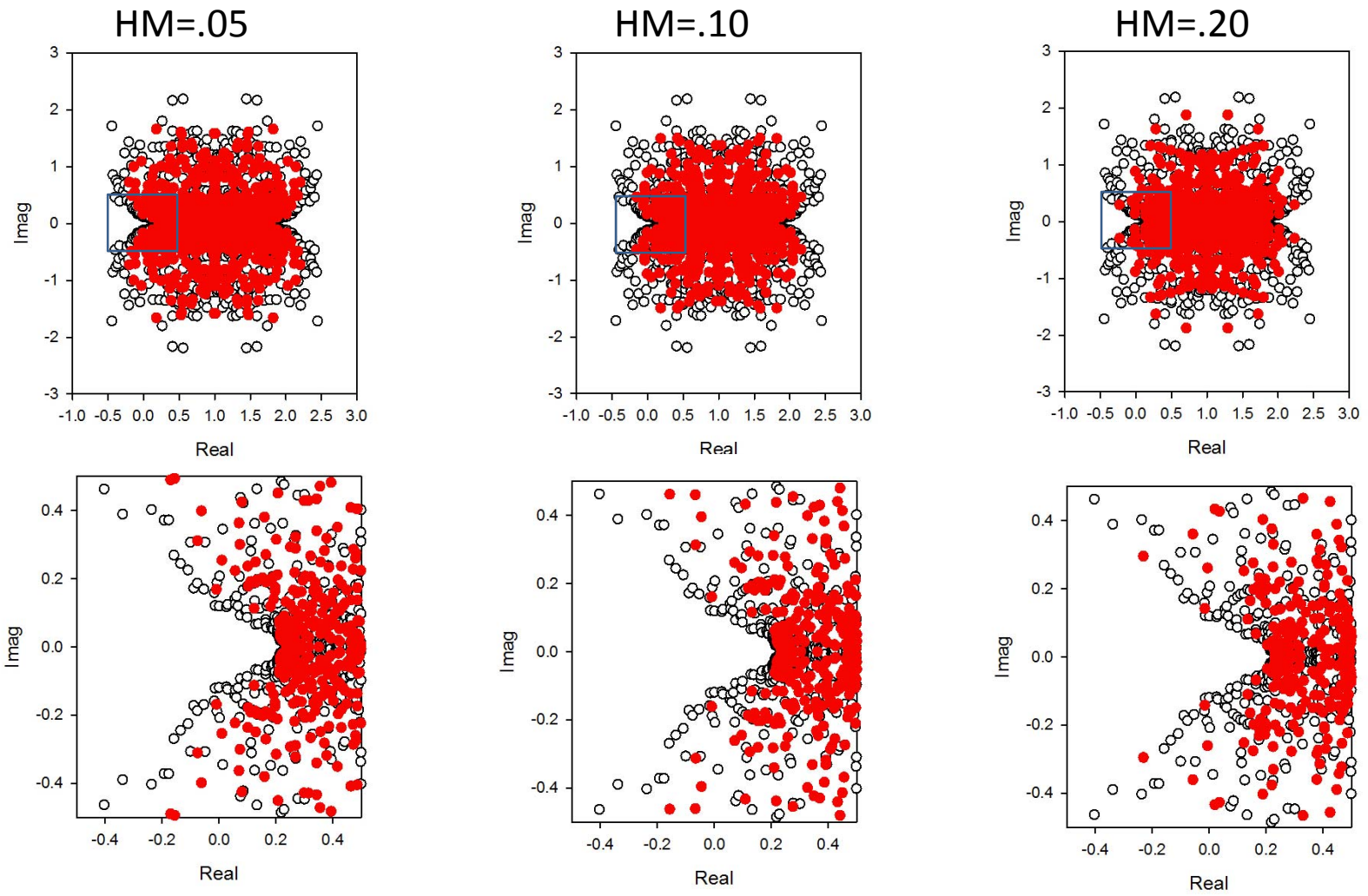

There is some improvement in the ratio of largest to smallest eigenvalues, but since matrix is non-symmetric, the significance of this is unclear.

Verification on 2D GEM Test Problem

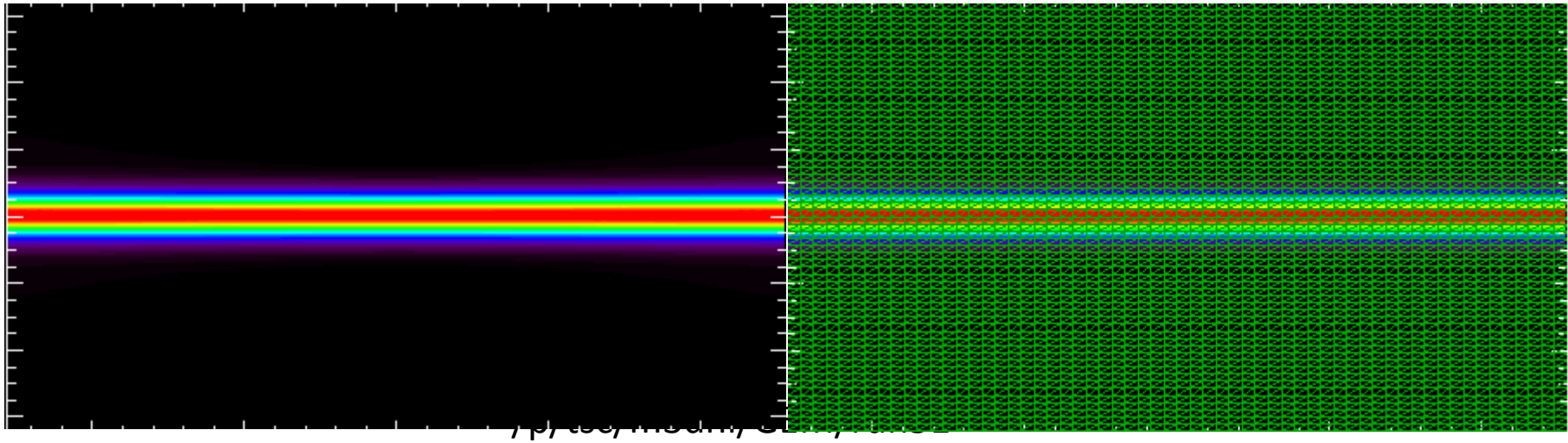

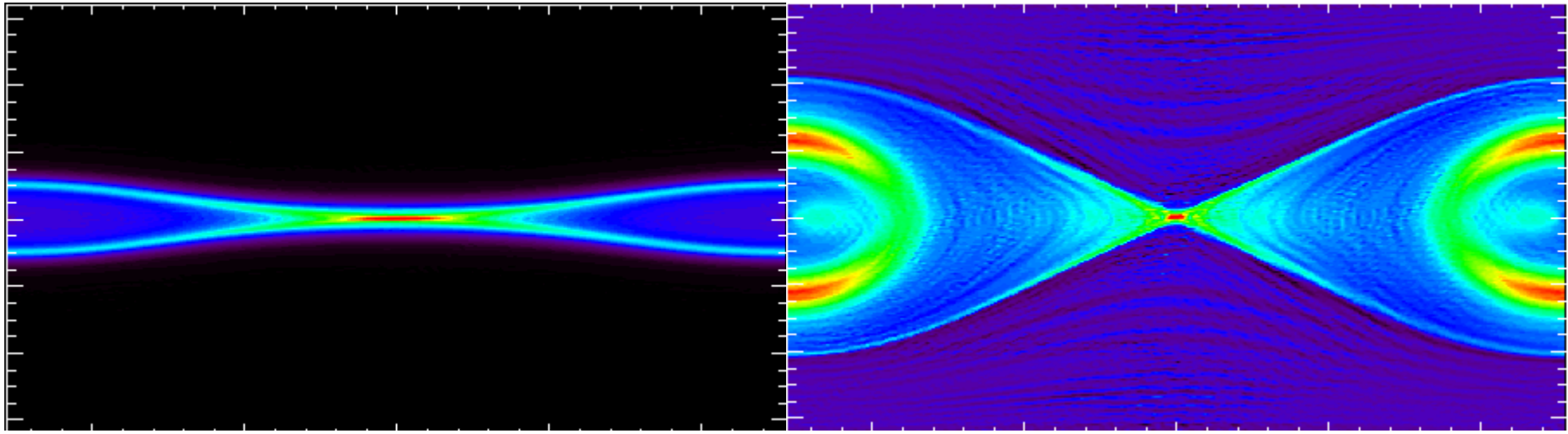

GEM Test Problem convergence study with and without new velocity operator

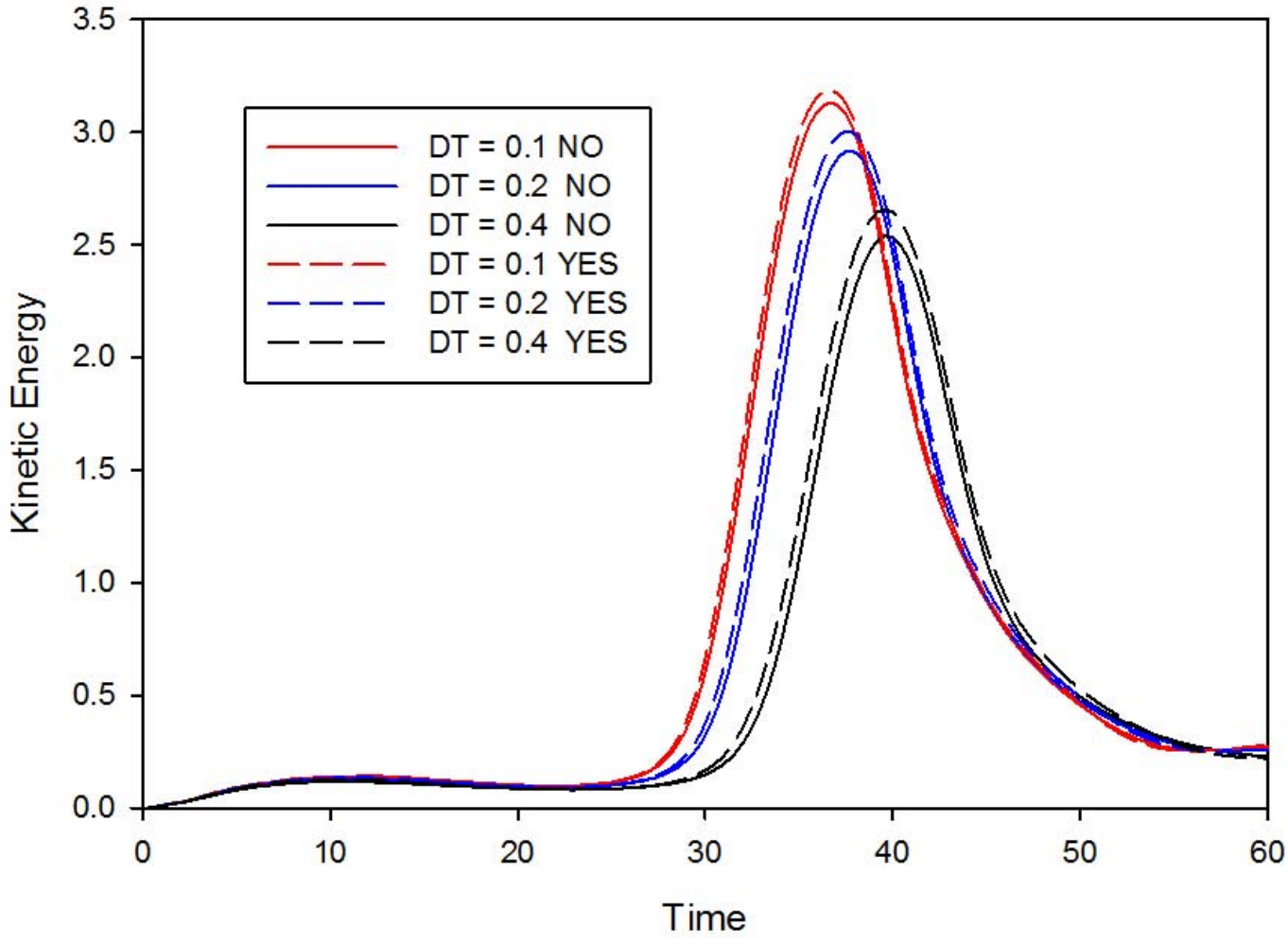

New terms appear to (slightly) improve time convergence!

Summary / Conclusions

- Sawtooth studies show wide range of behavior
  - Sawteeth, long-lived mode, snakes
- Actual evolution depends on many factors
  - Plasma boundary shape
  - Transport model and profile evolution
  - Heating and current drive terms
- Evidence that thermal crash time is separate from reconnection time and scales differently with resistivity.
- ITER studies show very little boundary distortion from internal mode
- Two-Fluid algorithm optimization underway
  - Comparing electron and ion form of Ohm's law
  - Optimizing 3D iterative solve